

An experiment on fabrication technique to establish three-dimensional curved surface of ETFE membrane structure by stretching cutting pattern strips

Quang Hieu BUI *1
Masaya KAWABATA *2

Synopsis

In the manufacture field of plastics, high strengthening by drawing of films is general. It is easy to draw uniaxial direction, however, there have been few cases that performed biaxial elongation, especially in three-dimensional (3D) shape. This paper presents an experiment of fabrication 3D curved surface of ETFE membrane structure by drawing the cutting pattern strips with several prescribed stress ratios between the warp or MD direction and the weft or TD direction. The results of the experiments showed that the 3D smooth curve surfaces could be established with the stress ratios as same as the prescribed stresses in form finding and cutting pattern analysis. In addition, the reduction of the rigidity of structures after the prestress construction period was seen at the pressure of around 1.3kPa.

1. Introduction

On the one hand, the final membrane structure shape is generally doubly curved surface, while the membrane material itself is manufactured in plane panels. Therefore, the cutting pattern is applied to divide the 3D curved surface into plane strips. In these procedures, the difference of the prescribed prestress state and the actual stress state in the structure can be occurred due to the material properties and numerical errors. To overcome this discrepancy, researchers focused on the optimization of cutting pattern with prescribed prestress [1][2] or introducing cutting pattern in form finding analysis [3][4].

On the other hand, the ETFE film is well used in membrane structures in recent years because of its advantages such as super lightweight, excellent light transmission, superior durability, self-cleaning properties and fire resistance performance etc. ETFE material itself had two yield points on its stress and strain curve [5], and the yield strength of ETFE film was increased by drawing the film to its plastic region [6]. The fabrication of low-rise 3D curved surface by drawing the plane film was confirmed by the authors' experiments. However, the establishment of high-rise 3D smooth curved surface by drawing the plane film still had problem because of the occurrence of wrinkling and insufficient prestress [7].

This paper presents the experiments to fabricate the 3D smooth curved surface of ETFE membrane structure by drawing the cutting

pattern strips. First, the form finding analysis is carried out with several prescribed stress ratios between the MD and TD directions. Second, the cutting pattern analysis based on the mathematical approach find the plane strips without the prestress which correspond to the results from the form finding. Third, these plane strips are connected by heat seal lines into the specimens, and the boundaries of these specimens are drawn to introduce the prestress of tension. The quantity of boundary extension guarantees the absence of wrinkling and the sufficiency of prestress. Finally, the pressurization test is carried out to confirm the strength of the ETFE structure after above construction stage. The results of the experiments showed that the 3D smooth curved surfaces could be established with the stress ratio between the MD and TD directions as approximate same as the prescribed stresses in form finding and cutting pattern analysis. And the reduction of the rigidity of structures after the prestress construction stage was seen at the pressure of around 1.3kPa.

2. Overview of experiments

2.1. The process of experiments

The experiments were carried out in three periods as shown in Fig. 1 as follow.

*1 Graduate student, Graduate School of Urban Innovation. Yokohama National University, Japan

*2 Associate Prof., Graduate School of Urban Innovation. Yokohama National University, Japan

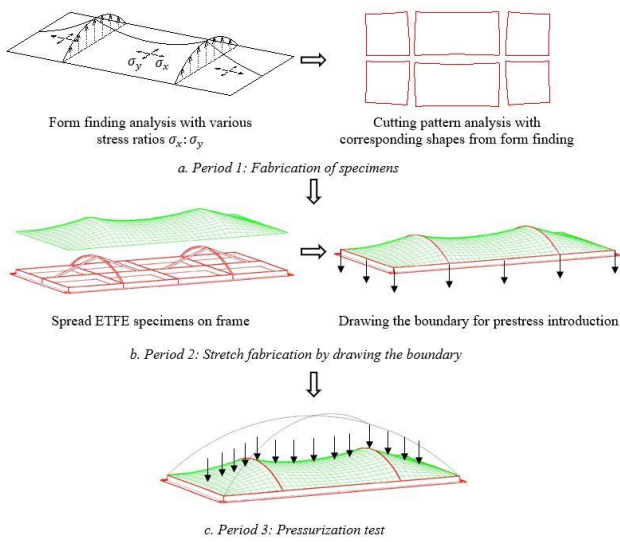


Fig.1 The process of experiments

The dimensions of the frame of experiments are shown in Fig.2, and all dimensions are in millimeter.

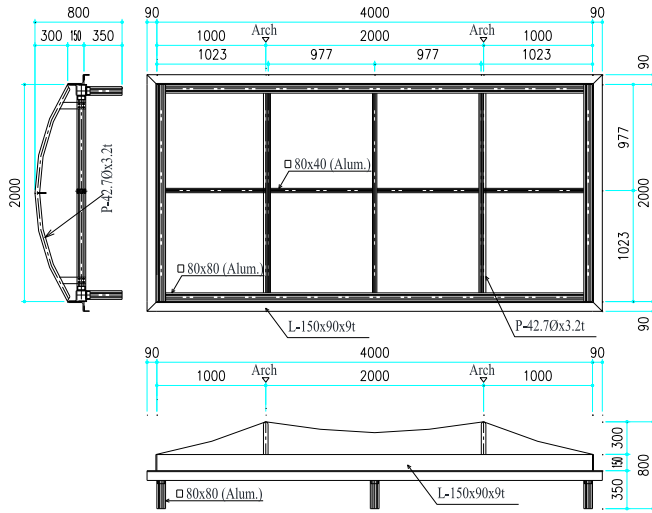


Fig.2 Dimensions of frame of experiments

2.2. Period 1: Fabrication of specimens

2.2.1. Form-finding analysis

In this paper, the MD direction is named as X direction, and the TD direction is named as Y direction. The isotropic stress surface method [8][9] was used for form finding in this paper. It is assumed that the membrane has a very small Young's modulus, and the initial stress ratios between the MD and TD directions are indicated in Fig.3. There were two types of specimens which are described in Table 1.

The results of form finding analysis are shown in Fig.4 in 3D view as well as in elevation view. The cutting pattern analysis is carried out to determine the dimensions of plane strips of the film which correspond to the shapes of form finding as shown in section 2.2.2.

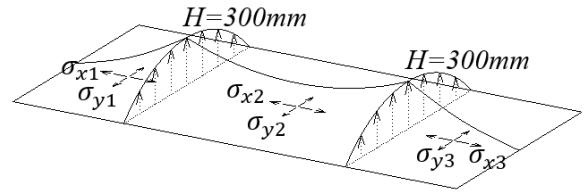


Fig.3 Assumptions for initial stress in form finding

Table 1. Types of specimens

Specimens	Stress ratios		
	$\sigma_{x1}: \sigma_{y1}$	$\sigma_{x2}: \sigma_{y2}$	$\sigma_{x3}: \sigma_{y3}$
DD301	3:1	1:1	3:1
DD302	3:1	3:1	3:1

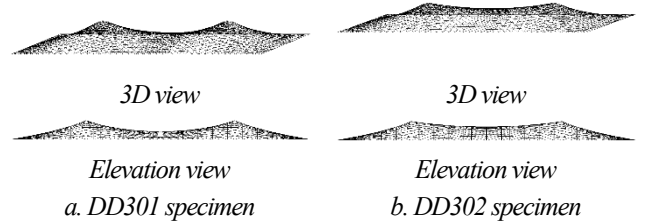


Fig.4 The results of form finding

2.2.2. Cutting pattern analysis

The least-squares minimization flattening approach [10] [11] was used in this paper for cutting pattern. The difference of the length between 3D coordinates and 2D coordinates is minimized by the equation Eq.1.

$$S(x) = \sum_{i=1}^m \phi_i^2(x) \quad (1)$$

where, m is the number of all link elements involved in plane strip, x is the coordinate vector of plane strip to be determined.

$$\phi_i = \sqrt{(x_{i,1} - x_{i,2})^2 + (y_{i,1} - y_{i,2})^2} - d_i \quad (2)$$

where, $(x_{i,1}, y_{i,1})$ and $(x_{i,2}, y_{i,2})$ are the unknown coordinates in the plane strip for the i th link element, and

$$d_i = \sqrt{(X_{i,1} - X_{i,2})^2 + (Y_{i,1} - Y_{i,2})^2 + (Z_{i,1} - Z_{i,2})^2} \quad (3)$$

is the actual length of the i th link element with 3D node coordinates $(X_{i,1}, Y_{i,1}, Z_{i,1})$ and $(X_{i,2}, Y_{i,2}, Z_{i,2})$ determined in the form finding procedure.

The results of these analyses are shown in Fig. 5.

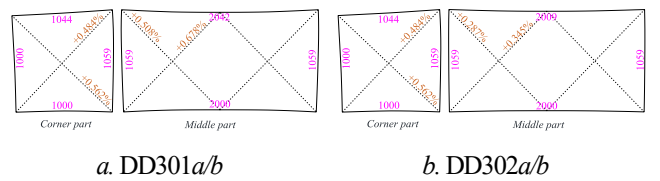


Fig.5 The cutting pattern shapes

In Fig.5, the numbers show the lengths of cutting lines, while the percentages indicate the expansions of the lengths of drape strips and the corresponding lengths of the form finding shapes. In this experiment, each type of cutting pattern shapes had two specimens named as DD301a/b and DD302a/b in the following parts.

2.3. Period 2: Stretch fabrication by drawing the boundary

After the specimens were spread out across the experiment frame, the boundaries of specimens were drawn by special technique which cannot be described in this paper. Fig.6a shows the values of drawing boundary in Z direction at four special positions in a quarter part of specimens, while the Fig.6b indicates that the values of drawing boundary are interpolated linearly at other positions of specimens.

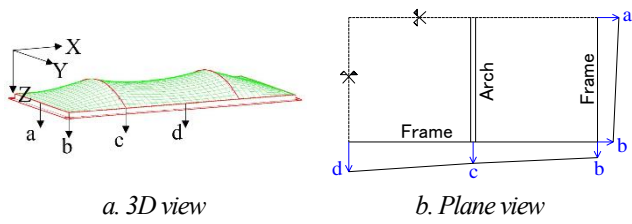


Fig.6 Process of drawing boundary

The experiments were carried out in five steps, and the values of drawing boundary are shown in Table 2.

Table 2. The process of experiments

	a (mm)	b (mm)	c (mm)	d (mm)
Step 1	0	0	0	0
Step 2	10	10	10	10
Step 3	20	15	20	20/25*
Step 4	30	20	30	30/40*
Step 5	40	30	40	40/50*

* The first value was used for DD301a/b, while the second value was used for DD302a/b

2.4. Period 3: Pressurization test

The pressurization test was carried out after around ten hours of stretch fabrication period. The process of pressure is described as follow: 0kPa → 0.5kPa → 0kPa → 1kPa → 0kPa → 1.5kPa → 0kPa → 2kPa → 0kPa.

3. Observation methods, results and discussions of experiments

3.1. Three-dimensional smooth curved surfaces

The 3D curved surfaces without wrinkling could be established by the suggested values of drawing boundary as shown in Table 2. Photo 1 presents the initial and final shapes throughout four specimens.

3.2. Saddle heights

The saddle heights of h_1 and h_2 , which are represented in Fig.7, are

measured by four laser displacement meters. The setup of laser displacement meters is shown in Fig. 8. In addition, those heights were also measured by the ruler at the first and final steps of experiments. The results of those heights are shown in Fig.9 regarding the target height of minimum surface.

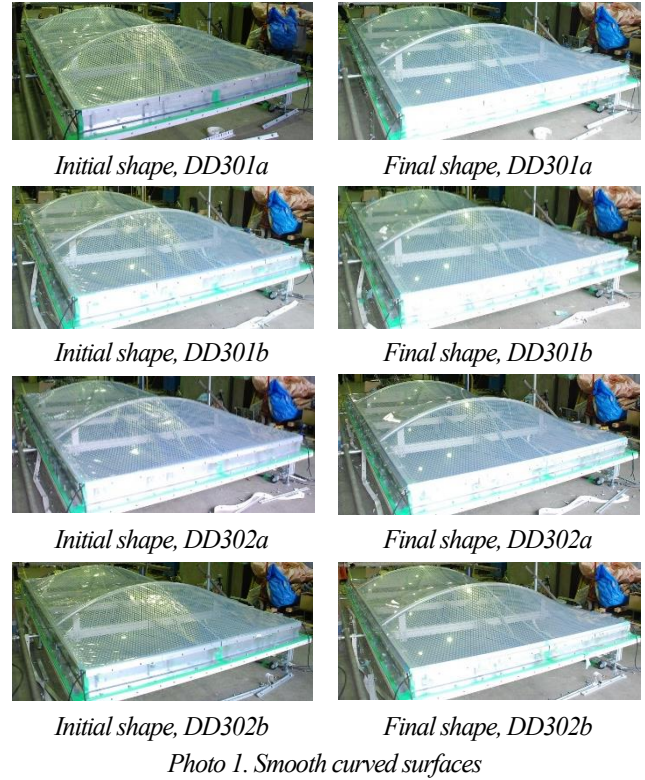


Photo 1. Smooth curved surfaces

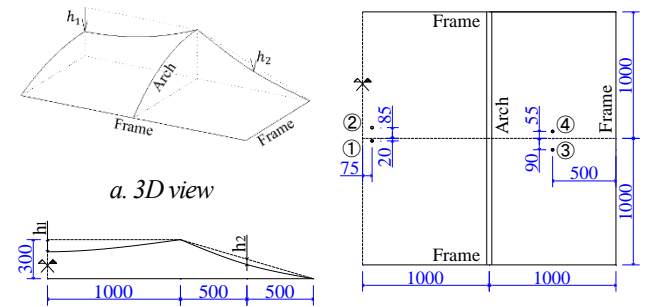


Fig.7 Saddle heights

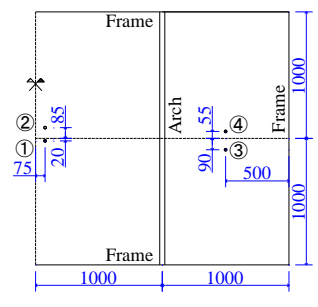


Fig.8 Setup of laser displacement meters

All dimensions are in millimeter

In Fig.9, while the dash lines show the results of hand measurement by ruler, the marked solid lines present the results of laser displacements meters. Moreover, solid lines without marker indicates the results of form finding in section 2.2.1 with stress ratio was 1:1 all over specimens. The saddle height h_1 of specimens DD301a/b at the final shape was higher than the results of minimum surface, while this height of specimens DD302a/b moved forward to the minimum surface results. Therefore, the prescribed stress ratios in form finding analysis should be chosen depended on the view points of architecture.

The saddle height h_2 of four specimens moved forward to the height of minimum surface. The stress ratio between MD and TD directions as 3:1 for the part between arches and frame were accepted highly.

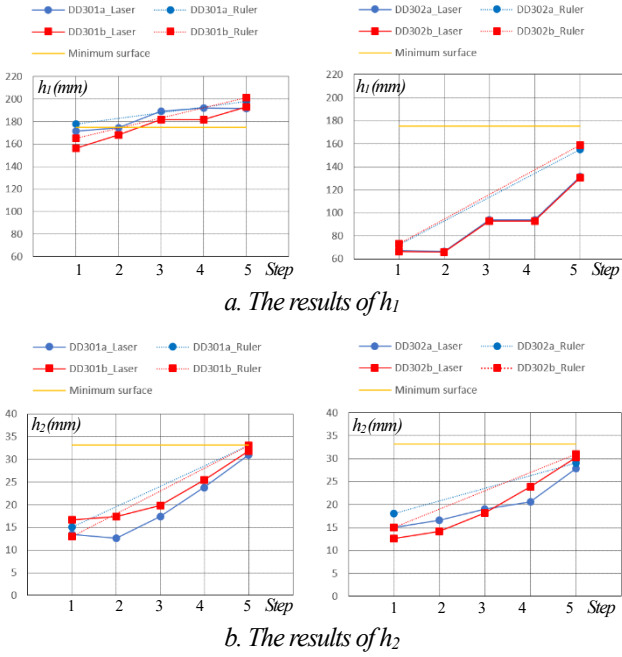


Fig.9 The results of saddle heights

3.3. Observed engineering strains

Four lengths shown in Fig. 10 were measured by tape measure with precision of 0.5mm during five steps of experiments. The engineering strains at step k are calculated by Eq. 4.

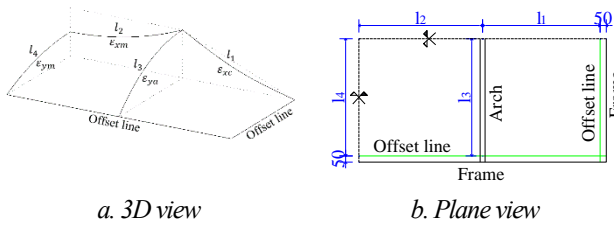


Fig.10 Observed four lengths

$${}_k \varepsilon = \frac{l_i - {}_k l_i}{l_i} \quad (4)$$

where, ${}_k \varepsilon$ is the engineering strain at step k , l_i and ${}_k l_i$ are the lengths of segment i at step l and step k , respectively. These strains are shown in the relation with the ratios between the boundary extension a , b , c or d and the span of structures in Fig.11.

In Fig.11, the solid lines with circle, square, triangle and diamond markers show the results of specimens DD301a, DD301b, DD302a and DD302b, respectively. In the part between two arches, the average ratio between ε_{xm} and ε_{ym} at the final step was 0.78 in case of DD301 and 2.87 in case of DD302. The suggested values of boundary extension kept the stress ratio between MD and TD directions as approximate same as the prescribed stress ratio in form finding and

cutting pattern analysis.

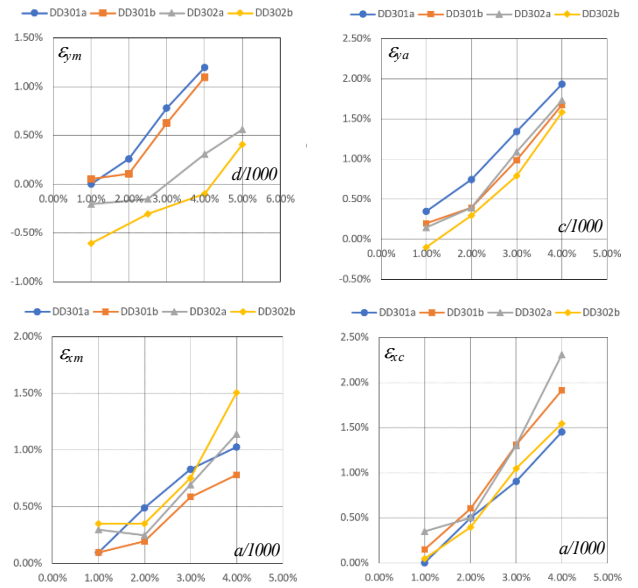


Fig.11 Observed engineering strains

The average ratio between ε_{xc} and ε_{xm} at the final step was 1.93 in case of DD301. This ratio was larger than the results of DD302 as 1.52. The reason can be explained by the effect of friction between arches and ETFE film. The saddle height h_1 of DD301 was higher than DD302, so the contact area between ETFE and arches in case of DD301 was larger than DD302. As a result, the contact angle in case of DD301 was larger than DD302. Summary, the above results can be understood clearly based on the belt friction theory [12].

3.4. Green-Lagrange strains at some parts on specimens

The lengths of four edges and two diagonals of part A and part B in Fig.12 were measured by paper tape and caliper during the experiments. The Green-Lagrange strains at those parts could be calculated based on the assumption that X direction is unchanged during the experiments. Fig. 13 indicates the assumption for this calculation.

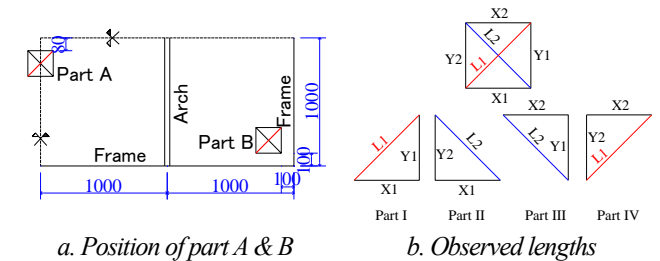


Fig.12 Observed lengths at part A&B

The Green-Lagrange strains can be obtained by Eq.5

$$\begin{Bmatrix} \varepsilon_x \\ \varepsilon_y \\ \varepsilon_{xy} \end{Bmatrix} = \frac{1}{2S} \begin{bmatrix} y_k - y_i & y_i - y_j & 0 \\ 0 & 0 & x_j - x_i \\ x_i - x_k & x_i - x_j & y_i - y_j \end{bmatrix} \begin{Bmatrix} u_j \\ u_k \\ v_k \end{Bmatrix} \quad (5)$$

where, $x_i = 0, y_i = 0, x_j = {}^1L_k, y_j = 0, x_k = {}^1L_j \cos(\alpha_l), y_k = {}^1L_j \sin(\alpha_l), u_j = {}^nL_k - {}^1L_k, u_k = {}^nL_j \cos(\alpha_n) - {}^1L_j \cos(\alpha_l), v_k = {}^nL_j \sin(\alpha_n) - {}^1L_j \sin(\alpha_l)$, and ${}^1L_k, {}^1L_j, {}^1L_k, {}^nL_k, \alpha_l, \alpha_n$ are described in Fig. 13.

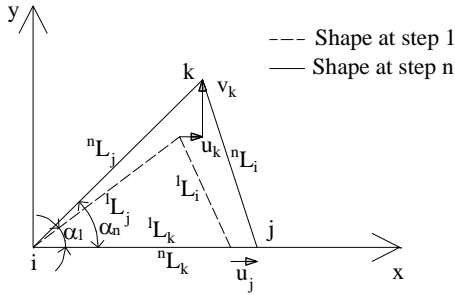
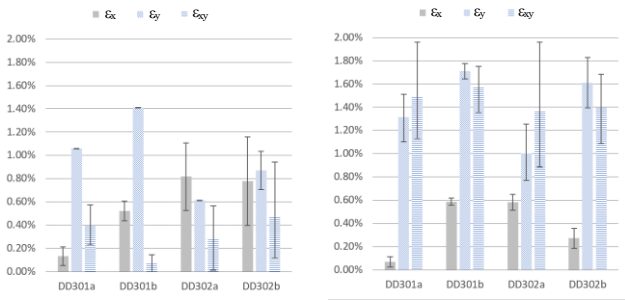


Fig.13 The assumptions for calculation of Green-Lagrange strains

Fig. 14 shows the results of Green-Lagrange strains of part A and B in the final step. The bar and error bars type of this graph indicates the average, maximum and minimum values of the strains at those parts.



a. Part A b. Part B
Fig.14 Green-Lagrange strains at part A&B

In Fig.14, the solid bar shows the strain in MD direction, while the diagonal pattern and horizontal pattern columns presents the strain in TD direction and the shear strain, respectively. At part A, strain in TD direction ϵ_y is around five times larger than strain in MD direction ϵ_x in case of DD301, while the MD and TD strains of DD302 are almost the same. The length of middle cutting pattern line was 2043mm for DD301 as shown in Fig.5. This length was larger than 2009mm of DD302. Therefore, the strain in MD direction ϵ_x of part A of DD302 was larger than DD301 with the same values of drawing boundary. The same phenomenon was observed in TD direction.

At part B, the drawing process must guarantee two criteria: (1) the ETFE will not be teared, (2) the wrinkling will not occur. As it can be seen in Fig.14b, although the shear strain at this part was large, the minimum principle strain was controlled to be larger than zeros at the final step. As a result, the smooth curved surface could be established with the suggested values of drawing boundary as shown in Table 2.

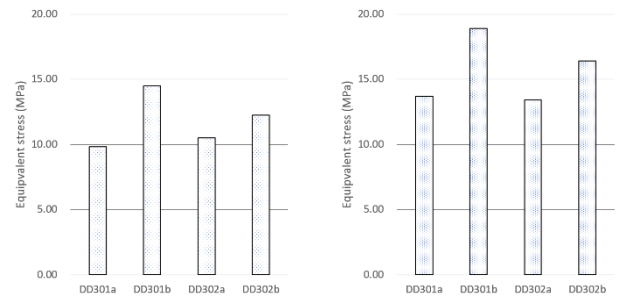
The 2nd Piola-Kirchhoff stresses of part A and part B can be obtained by Eq.6. Here, part A and part B were assumed in plane stress condition.

$$\begin{Bmatrix} S_x \\ S_y \\ S_{xy} \end{Bmatrix} = \frac{E}{1-\nu^2} \begin{bmatrix} 1 & \nu & 0 \\ \nu & 1 & 0 \\ 0 & 0 & \frac{1-\nu}{2} \end{bmatrix} \begin{Bmatrix} \epsilon_x \\ \epsilon_y \\ \epsilon_{xy} \end{Bmatrix} \quad (6)$$

where, $E=800MPa$ is Young modulus, and $\nu=0.44$ is Poisson's ratio of ETFE material. The equivalent stress is calculated by Eq.7.

$$S_{eq} = \sqrt{S_x^2 + S_y^2 - S_x S_y + 3S_{xy}^2} \quad (7)$$

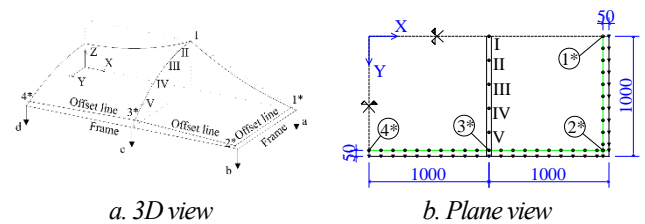
The average values of equivalent stress are shown in Fig.15. The equivalent stress of part A and part B was almost the same in both DD301 and DD302 specimens at the final step. Therefore, the described stress ratio in form finding and cutting pattern analysis can be chose either 3:1 or 1:1 for the middle part depended on the demand of saddle height h_1 .



a. Part A b. Part B
Fig.15 Equivalent stress at part A&B

3.5. Observed sliding values

During the experiments, the motions of marked points on specimens versus fixed points on frames and arches were measured by ruler with precision of 0.5mm. Fig.16 shows the positions of four special points on the offset lines of specimens and five points on specimens at the position of arch.



a. 3D view b. Plane view
Fig.16 Observed motion positions

The results of motions of four points (1* to 4*) versus boundary drawing values are shown in Fig. 17. In Fig.17, the solid lines with circle, square, triangle and diamond markers show the results of DD301a, DD301b, DD302a and DD302b, respectively. As we can see from Fig.17, the motion of the points on the offset lines are approximate a half of boundary drawing quantity.

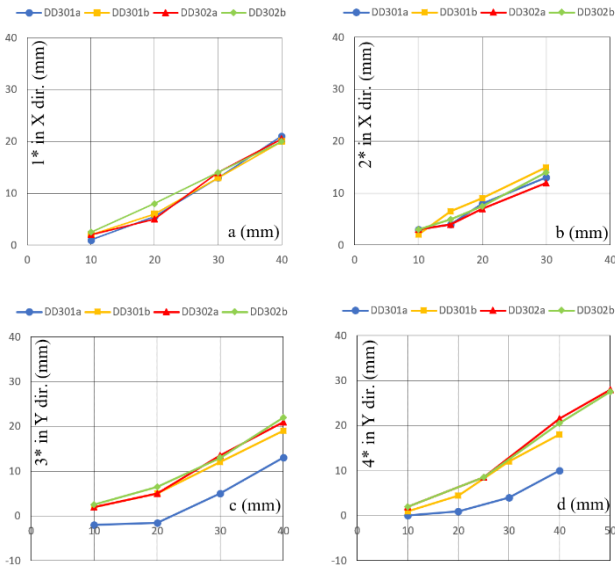


Fig.17 Motion of offset points

Fig.18 presents the motions of marked points on ETFE specimens versus the fixed points on arches in X and Y directions at the final step. It should be noted that the values of observed motions in Fig. 18 were measured on the curved of films in X direction and the curved of arches in Y direction by ruler with precision of $0.5mm$. The motion in Y direction was depended mainly on the boundary extension quantity at c position. The motion of the points near boundary were larger than the points in the middle of arches. In contrast, the motion in X direction was depended not only on the boundary extension quantity at a and d positions but also on the experiment process. Although the drawing process of boundary was carried out in order of c, a, d to b positions, this process could not take place similarly over four specimens. As a result, the motion in X direction at arches was different over four specimens.

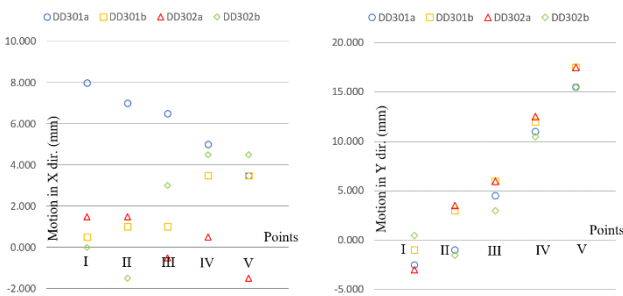


Fig.18 Motion at the position of arch

3.6. Pressurization test results

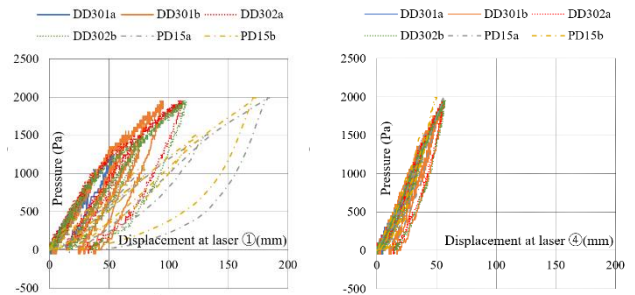
Photo 2 shows the shapes at the initial step of $0 kPa$ and final step of $2 kPa$. During the pressurization test, the vertical displacements at four positions in Fig. 8 were observed by laser displacement meters. The relations between the displacements at ① and ④ positions and pressure are presented in Fig. 19.



a. Initial shape at $0 kPa$ b. Final shape at $2 kPa$

Photo 2. Pressurization test, DD302b

In Fig. 19, the solid and dotted lines show the results of DD301, DD302 respectively, while the dot-and-dash lines present the results of PD15. It should be noted that PD15 were specimens which used flat type of cutting pattern in the part between two arches in previous experiments [7]. The residual displacements were observed at the pressure of $1.5kPa$ in both middle and corner parts over four specimens of DD301 and DD302. In addition, the reduction of the rigidity of structures can be seen at the pressure of $1.3kPa$ from those relation curve. In F19.a, the stiffness of the structures at the middle parts was larger than the previous experiments. The reason can be explained by the enough sufficient pre-stress of tension and the final smooth curved surface. In contrast, the stiffness of the structures at the corner parts was the same in both experiments because the same cutting pattern types were used in this part.



a. Middle part

b. Corner part

Fig.19 Relations between displacements and pressure

4. Conclusions

- (1) In tensile membrane structure using ETFE film, the form finding analysis can be carried out with several prescribed stress ratios between the MD and TD directions. Those ratios will be determined by the dimensions and the shapes of structures. The cutting pattern analysis based on the mathematical approach finds the cutting strips without the prestress consideration which correspond to the form finding results. The drape strips are connected by heat seal lines, and the boundary will be drawn to introduce the prestress. The 3D smooth curved surface with sufficient prestress could be established by those construction process.
- (2) The suggested values of boundary drawing can keep the stress ratio between MD and TD directions as approximate same as the prescribed stress ratio in form finding and cutting pattern analysis.

(3) The sufficient prestress could be confirmed not only by the engineering strains, the equivalent stress but also by the preservation of the rigidity of structures up to around 1.3 kPa of pressure.

Acknowledgements-The support for the experiments from Taiyo Kogyo Corporation is gratefully acknowledged.

References

- [1] M. Ohsaki, K. Uetani: Shape-stress trade-off design of membrane structures for specified sequence of boundary shapes, *Comput. Methods Appl. Mech. Engrg.* 182(2000), pp. 73-88
- [2] Jae-Yeol Kim, Jang-Blog Lee: A new technique for optimum cutting pattern generation of membrane structure, *Engineering Structures* 24(2002), pp. 745-756
- [3] J. Linhard, R. Wuchner and K. Bletzinger: Introducing cutting pattern in form finding and structural analysis, *Textile Composites and Inflatable Structure II*, 2008, pp. 69-84
- [4] Kazuo Ishii: Form finding analysis in consideration of cutting patterns of membrane structures, *International Journal of Space Structures* Vol.14, No.2, 1999, pp.105-119
- [5] M. Kawabata, E. Jeong and K. Nishikawa: Curved surface fabrication and strengthening of film structures by stretching plane film, *Proceedings of IASS Symposium*, 2008
- [6] E. Jeong and M. Kawabata: An Experimental and Analytical Study on Stretching Effect of ETFE film, *Research Report on Membrane Structures*, 2014
- [7] E. Ishida, Q.H. Bui and M. Kawabata: Study on fabrication of film panel of parallel arch model by 3D composite cutting pattern, *AJ 2017 conference*, pp.739-740 (in Japanese).
- [8] B. Tabarrok, Z. Qin: Nonlinear analysis of tension structures, *Computers and Structures* Vol.45, No.5/6, pp. 973-984, 1992
- [9] Kazuo Ishii: State of the art report on form finding problem of membrane structures, *Research Report on Membrane Structures*, 1990
- [10] B. Tabarrok, Z. Qin: Form finding and cutting pattern generation for fabric tension structures, *Microcomputers in Civil Engineering* 8, 1993, pp. 377-384
- [11] Jae-Yeol Kim, Jang-Bog Lee: A new technique for optimum cutting pattern generation of membrane structures, *Engineering structures* 24, 2002, pp. 745-756
- [12] Stephen W. Attaway: The mechanics of friction in rope rescue, *International Technical Rescue Symposium*, 1999

裁断図を延伸して ETFE 膜構造の 3 次元曲面を成形するための作製技術に関する実験的研究

BUI Quang Hieu *1)
河端 昌也 *2)

梗概

塑性範囲の製造分野では、フィルムの延伸による高強度化が一般的である。一軸方向を引張することは容易であるが、特に三次元 (3D) 形状で二軸引張を行うケースはほとんどない。本研究では、縦糸方向または MD 方向と横糸方向または TD 方向の様々な定める応力比で複合立体裁断を延伸することにより、ETFE 膜構造の 3 次元曲面加工を実験した。実験の結果は、形状解析および裁断解析における規定された応力と同じ応力比で 3D 滑らかな曲面を確立できることを示した。加えて、延伸形成実験の後は構造の剛性の低下は、約 1.3kPa の圧力で見られた。

*1) 横浜国立大学大学院 都市イノベーション学府 大学院生

*2) 横浜国立大学大学院 都市イノベーション研究院 准教授